Research Square

Preprints are preliminary reports that have not undergone peer review.
They should not be considered conclusive, used to inform clinical practice,
or referenced by the media as validated information.

Conventional time series, machine and deep learning approaches for rainfall forecasting in a bimodal climate in Embu County, Kenya: A comparative study of SARIMA, ANN, LSTM, CNN and hybrid models

Robert Mutwiri

rmutwiri@seku.ac.ke

South Eastern Kenya University

Joel Ngesa

South Eastern Kenya University

Mary Mwangi

South Eastern Kenya University

Mark Kimathi

Machakos University

Research Article

Keywords: Rainfall forecasting, SARIMA, LSTM, CNN--LSTM, Hybrid deep learning models

Posted Date: May 26th, 2026

DOI: https://doi.org/10.21203/rs.3.rs-9725114/v1

License: This work is licensed under a Creative Commons Attribution 4.0 International License.
Read Full License

Additional Declarations: No competing interests reported.

Conventional time series, machine and deep learning approaches for rainfall forecasting in a bimodal climate in Embu County, Kenya: A comparative study of SARIMA, ANN, LSTM, CNN and hybrid models

Robert Mutwiri[1*], Joel Ngesa[1†], Mary Mwangi[2†], Mark Kimathi[3†]

[1*]Department of Mathematics and Actuarial Science, South Eastern University Kenya, P.O Box 170,Kitui, 90200, Kenya.
[2]Department of Geology and Meteorology, South Eastern University Kenya, P.O Box 170, City, 90200, Kenya.

*Corresponding author(s). E-mail(s): rmutwiri@seku.ac.ke;
Contributing authors: nochola@seku.ac.ke; wmwangi@seku.ac.ke;
mark.kimathi@mksu.ac.ke;
†These authors contributed equally to this work.

Abstract

Accurate rainfall forecasting is critical for agricultural planning, water resource management, and climate risk reduction in regions characterized by strong seasonal variability and nonlinear climatic behaviour. This study evaluates the predictive performance of statistical, machine learning, and hybrid deep learning models for monthly rainfall forecasting in Embu County, Kenya, using data from 1998 to 2025 obtained from the Kenya Meteorological Department. The rainfall series exhibits a bimodal structure with moderate variability (CV = 7.08%), slight negative skewness, and near-normal distributional characteristics. Stationarity and diagnostic tests confirm suitability for time series modelling. The optimal linear benchmark model is identified as SARIMA$\mathbf{(1,1,1)(0,1,1)_{12}}$ based on information criteria; however, its forecasting ability is limited in capturing nonlinear rainfall dynamics. To improve predictive accuracy, Artificial Neural Network (ANN), Long Short-Term Memory (LSTM), and hybrid models including SARIMA–ANN, SARIMA–LSTM, SARIMA–NNAR–LSTM, and SARIMA–CNN–LSTM are developed. Model evaluation is conducted using

RMSE, MAE, and MSE under both training and testing frameworks, complemented by residual diagnostics and Diebold–Mariano tests. Results show that hybrid models consistently outperform standalone approaches. The SARIMA–CNN–LSTM model achieves the best performance with RMSE = 1.68, MAE = 1.30, and MSE = 2.82, along with the smallest training–testing gap, indicating strong generalization and minimal overfitting. Residual diagnostics confirm near white-noise behavior for hybrid models, while Diebold–Mariano tests indicate statistically significant improvements over SARIMA at the 5% level. Overall, the findings demonstrate that rainfall variability in Embu County is driven by interacting linear seasonal, nonlinear, and long-memory processes. Hybrid deep learning frameworks, particularly CNN–LSTM-based models, provide a robust and reliable approach for rainfall forecasting in bimodal climatic systems.

Keywords: Rainfall forecasting; SARIMA; LSTM; CNN–LSTM; Hybrid deep learning models

1 Introduction

Rainfall variability remains a major environmental and socio-economic challenge in sub-Saharan Africa, where agriculture, water resource management, food security, and flood preparedness largely depend on reliable forecasts under highly variable hydro-climatic regimes, since rainfall is a critical climatic factor influencing livelihoods and socio-economic activities in predominantly rain-fed communities [16, 48]. In Kenya, increasing climate variability has intensified rainfall irregularities, resulting in recurrent droughts, floods, crop failures, and food insecurity [2, 14]. Embu County, located on the southeastern slopes of Mount Kenya, experiences a bimodal rainfall regime characterized by long rains (MAM) and short rains (OND). However, recent climatic changes have increased rainfall uncertainty through delayed onset, shortened seasons, and intensified extreme rainfall events [17]. These variations are strongly influenced by large-scale climate drivers such as the El Niño–Southern Oscillation (ENSO) and the Indian Ocean Dipole (IOD) [2, 25, 26]. Consequently, accurate rainfall forecasting is critical for agricultural planning, hydrological management, and climate risk mitigation [19].

Conventional statistical approaches such as Seasonal Autoregressive Integrated Moving Average (SARIMA) models have been widely applied in meteorological and climate change forecasting research because of their effectiveness in capturing linear trends, seasonal structures, and temporal dependencies inherent in rainfall time series data[20, 40]. However, rainfall processes are inherently nonlinear, stochastic, and highly dynamic, thereby limiting the predictive capability of purely linear models in complex climatic systems [15, 24, 47]. To address these limitations, machine learning and deep learning methods including Artificial Neural Networks (ANNs) and Long Short-Term Memory (LSTM) networks have gained increasing attention because of their ability to model nonlinear relationships and long-term temporal dependencies [3, 9, 11, 46]. Empirical evidence suggests that deep learning architectures frequently outperform traditional statistical methods in climate and hydrological forecasting

applications due to their superior ability to capture nonlinear patterns and long-term temporal dependencies [32, 33, 36, 46].

Despite these advances, standalone machine learning models may inadequately capture strong seasonal rainfall structures and may suffer from instability or overfitting when applied independently to highly seasonal climatic time series [5, 35, 47]. Consequently, recent forecasting research has shifted toward hybrid statistical–deep learning frameworks that integrate the strengths of statistical decomposition and nonlinear learning [5, 6, 47]. Hybrid approaches allow statistical models to capture linear seasonality while deep learning architectures model nonlinear residual structures and hidden temporal dynamics, thereby improving forecasting accuracy and model robustness [5, 6, 31, 47].

In Kenya, several studies have examined rainfall variability at the national scale, with a general consensus indicating increasing temporal and spatial rainfall variability across the country [29, 30, 40]. These studies report increasing frequency of extreme wet and dry events, shifting seasonal rainfall patterns, and growing climatic uncertainty. However, relatively few studies have focused on regional or county-level rainfall dynamics, despite the importance of localized climatic analysis for supporting evidence-based policy formulation, agricultural planning, and climate adaptation strategies [28, 29].

This study develops and systematically evaluates advanced hybrid forecasting frameworks for monthly rainfall prediction in Embu County, Kenya. Specifically, conventional statistical, machine learning, deep learning, and hybrid architectures including SARIMA, ANN, LSTM, SARIMA–ANN, SARIMA–LSTM, SARIMA–NNAR–LSTM, and SARIMA–CNN–LSTM are comparatively assessed under a unified experimental framework. This study introduces a multi-stage hybrid rainfall forecasting framework that integrates SARIMA-based seasonal decomposition, CNN feature extraction, NNAR nonlinear learning, and LSTM temporal memory to jointly capture linear, nonlinear, and long-range dependencies in rainfall time series. It further contributes a standardized benchmarking design with identical datasets and evaluation protocols, enabling fair and reproducible comparison across statistical, deep learning, and hybrid forecasting models.

The rest of the paper is organized as follows: Section 2 presents the literature review, Section 3 methodology, Section 4 Results, Section 5 discussion, and Section 6 concludes the study.

2 Materials and Methods

2.1 Data and Data Source

The study was conducted in Embu County, Kenya, located on the eastern slopes of Mount Kenya between latitudes $0°8'$ and $0°50'$ South and longitudes $37°3'$ and $37°9'$ East. The region experiences a bimodal rainfall pattern, with long rains occurring from March to May and short rains from October to December. Agriculture is the main economic activity in the county, making rainfall variability a critical factor influencing food security, water availability, and livelihoods. Secondary monthly rainfall data for the period 1998 to 2025 were obtained from the Kenya Meteorological Department

(KMD), Embu station. The dataset comprised total monthly rainfall measured in millimeters (mm). The data were organized as a univariate time series with a frequency of 12 observations per year to capture seasonal patterns and support forecasting analysis.

2.2 Statistical models

2.2.1 SARIMA Model

The Seasonal Autoregressive Integrated Moving Average (SARIMA) model is defined as SARIMA$(p, d, q)(P, D, Q)_s$, where s is the seasonal period. The general form is given by:

$$\Phi_p(B)\Phi_P(B^s)(1-B)^d(1-B^s)^D y_t = \Theta_q(B)\Theta_Q(B^s)\varepsilon_t$$

where B is the backshift operator, $\Phi_p(B)$ and $\Phi_P(B^s)$ represent non-seasonal and seasonal autoregressive polynomials, $\Theta_q(B)$ and $\Theta_Q(B^s)$ represent non-seasonal and seasonal moving average polynomials, and ε_t is a white noise error term with zero mean and constant variance.

The SARIMA model assumes that rainfall at time t is a linear combination of its past values and past error terms, incorporating both seasonal and non-seasonal structures.

2.3 Machine Learning Models

2.3.1 Artificial Neural Network (ANN) Model

Let $\{x_t\}_{t=1}^T$ denote an input vector constructed from lagged observations of a rainfall time series, such that:

$$\mathbf{x}_t = (y_{t-1}, y_{t-2}, \ldots, y_{t-n})^T$$

where n is the number of lagged inputs.

The Artificial Neural Network (ANN) is a nonlinear function approximator that learns a mapping:

$$f_\theta : \mathbb{R}^n \to \mathbb{R}, \quad \hat{y}_t = f_\theta(\mathbf{x}_t)$$

where θ represents the set of all network parameters (weights and biases).

For a feedforward neural network with one hidden layer, the hidden layer transformation is defined as:

$$\mathbf{z}_t = \phi\left(W^{(1)}\mathbf{x}_t + \mathbf{b}^{(1)}\right)$$

where $W^{(1)}$ is the weight matrix, $\mathbf{b}^{(1)}$ is the bias vector, and $\phi(\cdot)$ is a nonlinear activation function such as ReLU or sigmoid.

The output layer is given by:

$$\hat{y}_t = W^{(2)}\mathbf{z}_t + b^{(2)}$$

Combining these expressions, the ANN model can be written as a nested nonlinear function:

$$\hat{y}_t = W^{(2)}\,\phi\left(W^{(1)}\mathbf{x}_t + \mathbf{b}^{(1)}\right) + b^{(2)}$$

More generally, for a deep neural network with L layers, the recursive representation is:

$$\mathbf{a}^{(l)} = \phi\left(W^{(l)}\mathbf{a}^{(l-1)} + \mathbf{b}^{(l)}\right), \quad l = 1, 2, \ldots, L$$

with $\mathbf{a}^{(0)} = \mathbf{x}_t$ and output:

$$\hat{y}_t = \mathbf{a}^{(L)}$$

The ANN is trained by minimizing a loss function over all observations:

$$\min_{\theta} \frac{1}{T}\sum_{t=1}^{T}(y_t - \hat{y}_t)^2$$

Parameter optimization is performed using gradient-based learning methods such as stochastic gradient descent (SGD) or Adam, with gradients computed via backpropagation:

$$\theta \leftarrow \theta - \eta\frac{\partial \mathcal{L}}{\partial \theta}$$

where η is the learning rate and $\mathcal{L}$ is the loss function.

2.3.2 Long Short-Term Memory (LSTM) Model

Let $\{x_t\}_{t=1}^{T}$ denote an input sequence, and let $\{h_t\}_{t=1}^{T}$ represent the corresponding hidden states of a recurrent neural network. Standard recurrent neural networks suffer from vanishing and exploding gradient problems, limiting their ability to capture long-term dependencies. The Long Short-Term Memory (LSTM) network addresses this limitation through a gated memory cell structure.

The LSTM maintains a cell state C_t, which acts as an internal memory, and a hidden state h_t, which represents the output at time t. The evolution of these states is governed by gating mechanisms.

Forget gate:

$$f_t = \sigma\left(W_f[h_{t-1}, x_t] + b_f\right)$$

which determines the proportion of previous memory C_{t-1} to retain.

Input gate:

$$i_t = \sigma\left(W_i[h_{t-1}, x_t] + b_i\right)$$

which controls the amount of new information to be added.

Candidate memory state:

$$\tilde{C}_t = \tanh\left(W_c[h_{t-1}, x_t] + b_c\right)$$

Cell state update:

$$C_t = f_t \odot C_{t-1} + i_t \odot \tilde{C}_t$$

where $\odot$ denotes element-wise multiplication.

Output gate:

$$o_t = \sigma\left(W_o[h_{t-1}, x_t] + b_o\right)$$

Hidden state update:

$$h_t = o_t \odot \tanh(C_t)$$

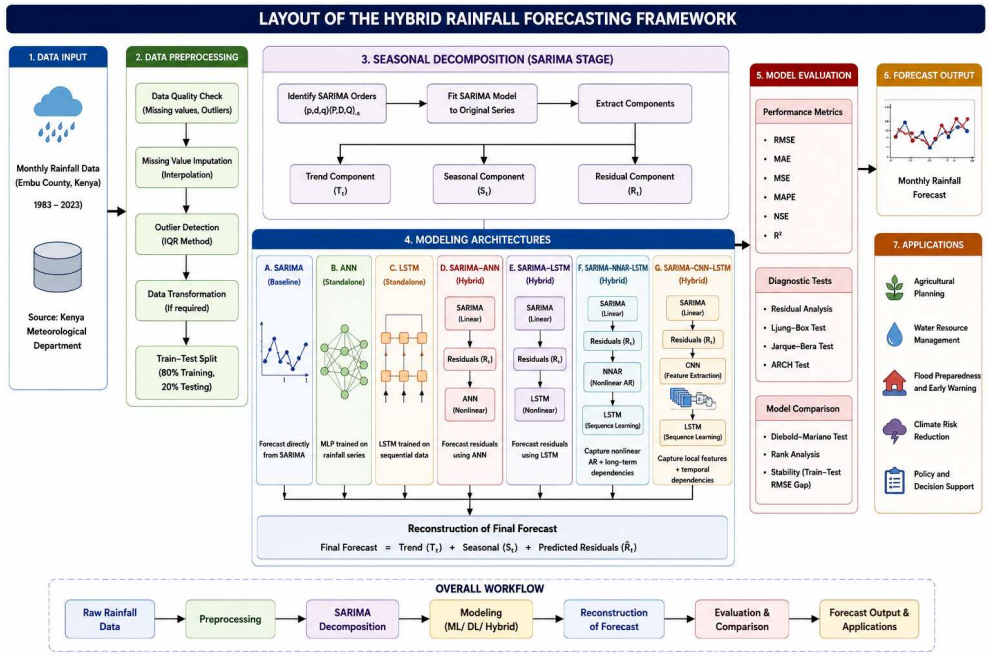


Fig. 1 Layout of the unified hybrid rainfall forecasting framework showing the sequential workflow from rainfall data acquisition and preprocessing to SARIMA-based seasonal decomposition, standalone and hybrid model development, model evaluation, residual diagnostics, forecast generation, and climate-related applications. The framework integrates statistical, machine learning, and deep learning architectures, including SARIMA, ANN, LSTM, SARIMA–ANN, SARIMA–LSTM, SARIMA–NNAR–LSTM, and SARIMA–CNN–LSTM, to capture linear seasonality, nonlinear rainfall variability, localized feature patterns, and long-term temporal dependencies for improved rainfall forecasting accuracy in bimodal climatic systems.

The LSTM network defines a nonlinear state-space mapping:

$$h_t = \mathcal{F}_\theta(x_t, h_{t-1}, C_{t-1})$$

where $\mathcal{F}_\theta(\cdot)$ represents the parameterized LSTM transformation.

Given a target sequence $\{y_t\}$, the LSTM is trained by minimizing the empirical loss function:

$$\min_\theta \sum_{t=1}^{T} (y_t - \hat{y}_t)^2$$

Training is performed using Backpropagation Through Time (BPTT), allowing gradients to propagate across temporal steps while mitigating vanishing gradient issues through gated memory control.

2.4 Hybrid Modeling Approach

Hybrid forecasting models integrate statistical time series methods and machine learning techniques to capture both linear and nonlinear structures in complex and non-stationary climate systems. In rainfall forecasting, Seasonal Autoregressive Integrated Moving Average (SARIMA) models are effective in modeling linear trends and seasonal patterns, while machine learning models such as Artificial Neural Networks (ANN) and Long Short-Term Memory (LSTM) networks capture nonlinear dependencies and higher-order interactions in the data.

In this study, hybrid models are constructed using a residual decomposition framework. The SARIMA model is first used to extract the linear and seasonal structure of the rainfall series. Let the observed rainfall be denoted by y_t and the SARIMA forecast by $\hat{y}_t^{(S)}$. The residual component is defined as:

$$e_t = y_t - \hat{y}_t^{(S)}$$

These residuals represent the nonlinear and unexplained dynamics of the series and are subsequently modeled using machine learning methods.

2.4.1 Hybrid SARIMA–ANN Model

Let $\{y_t\}_{t=1}^{T}$ denote a univariate rainfall time series. The SARIMA model is used to decompose the series into a linear seasonal component and a stochastic residual component.

The SARIMA$(p, d, q)(P, D, Q)_s$ model can be written as:

$$y_t = L_t + \varepsilon_t$$

where L_t represents the linear seasonal structure captured by the SARIMA model, and ε_t is a zero-mean white noise process.

Equivalently, the SARIMA model produces an optimal linear forecast:

$$\hat{y}_t^{(S)} = \mathbb{E}(y_t \mid \mathcal{F}_{t-1})$$

where $\mathcal{F}_{t-1}$ is the information set up to time $t-1$.

The corresponding residual series is defined as:

$$e_t = y_t - \hat{y}_t^{(S)}$$

This residual contains nonlinear dynamics not captured by the linear SARIMA structure. We assume:

$$e_t = g(\mathbf{x}_t) + \eta_t$$

where $g(\cdot)$ is an unknown nonlinear function, $\mathbf{x}_t = (e_{t-1}, e_{t-2}, \ldots, e_{t-n})$ is the lagged residual vector, and η_t is an irreducible error term.

To approximate $g(\cdot)$, an Artificial Neural Network (ANN) is employed as a universal function approximator:

$$\hat{e}_t^{(ANN)} = f_\theta(\mathbf{x}_t)$$

where $f_\theta(\cdot)$ represents the ANN with parameters θ.

A standard feedforward ANN with one hidden layer can be expressed as:

$$\hat{e}_t^{(ANN)} = \sigma\left(W^{(2)}\,\phi(W^{(1)}\mathbf{x}_t + b^{(1)}) + b^{(2)}\right)$$

where $\phi(\cdot)$ and $\sigma(\cdot)$ are activation functions.

The ANN is trained by minimizing the empirical risk:

$$\min_\theta \sum_{t=1}^{T}\left(e_t - \hat{e}_t^{(ANN)}\right)^2$$

The final SARIMA?ANN hybrid forecast is obtained by additive decomposition:

$$\hat{y}_t = \hat{y}_t^{(S)} + \hat{e}_t^{(ANN)}$$

Substituting the definitions gives:

$$\hat{y}_t = \mathbb{E}(y_t \mid \mathcal{F}_{t-1}) + f_\theta(y_t - \mathbb{E}(y_t \mid \mathcal{F}_{t-1}))$$

The hybrid model decomposes rainfall dynamics into a linear conditional expectation estimated by SARIMA and a nonlinear correction term learned by ANN. This results in a semi-parametric forecasting structure capable of capturing both seasonal linear dependence and nonlinear residual behavior.

2.4.2 Hybrid SARIMA–LSTM Model

Let $\{y_t\}_{t=1}^T$ denote a univariate rainfall time series. The SARIMA model is first used to extract the linear and seasonal structure of the process. The SARIMA forecast is defined as the conditional expectation:

$$\hat{y}_t^{(S)} = \mathbb{E}(y_t \mid \mathcal{F}_{t-1})$$

where $\mathcal{F}_{t-1}$ represents the information set up to time $t-1$.

The observed series is decomposed into:

$$y_t = \hat{y}_t^{(S)} + e_t$$

where e_t denotes the residual component capturing nonlinear and non-seasonal dynamics not explained by the SARIMA structure.

To model the residual process, we assume that e_t follows an unknown nonlinear autoregressive structure:

$$e_t = g(e_{t-1}, e_{t-2}, \ldots, e_{t-n}) + \eta_t$$

where $g(\cdot)$ is an unknown nonlinear function and η_t is an irreducible noise term.

A Long Short-Term Memory (LSTM) network is employed to approximate $g(\cdot)$ due to its ability to model long-term dependencies in sequential data. The LSTM learns a functional mapping:

$$\hat{e}_t^{(LSTM)} = f_\theta(e_{t-1}, e_{t-2}, \ldots, e_{t-n})$$

where $f_\theta(\cdot)$ represents the LSTM parameterized by θ.

The internal LSTM dynamics are governed by the gating mechanism:

$$f_t = \sigma(W_f[h_{t-1}, e_t] + b_f), \quad i_t = \sigma(W_i[h_{t-1}, e_t] + b_i)$$

$$\tilde{C}_t = \tanh(W_c[h_{t-1}, e_t] + b_c)$$
$$C_t = f_t C_{t-1} + i_t \tilde{C}_t$$
$$h_t = o_t \tanh(C_t)$$

The LSTM parameters are estimated by minimizing the empirical loss function:

$$\min_\theta \sum_{t=1}^{T} \left(e_t - \hat{e}_t^{(LSTM)}\right)^2$$

Finally, the SARIMA–LSTM hybrid forecast is obtained by combining the linear SARIMA component and the nonlinear LSTM component:

$$\hat{y}_t = \hat{y}_t^{(S)} + \hat{e}_t^{(LSTM)}$$

2.5 Hybrid SARIMA–NNAR–LSTM Model

The SARIMA–NNAR–LSTM hybrid framework integrates statistical time series modelling with nonlinear neural networks and recurrent deep learning to capture both seasonal linear dynamics and complex nonlinear temporal dependencies in rainfall data. Let $\{y_t\}$ denote the observed rainfall series.

The SARIMA component models the linear and seasonal structure as:

$$\Phi_P(B^s)\phi_p(B)(1-B)^d(1-B^s)^D y_t = \Theta_Q(B^s)\theta_q(B)\varepsilon_t, \tag{1}$$

where B is the backshift operator, s is the seasonal period, and ε_t is white noise. The SARIMA forecast is denoted by $\hat{y}_t^{(S)}$, and the residuals are defined as:

$$r_t = y_t - \hat{y}_t^{(S)}. \tag{2}$$

To model nonlinear structures in the residuals, a NNAR model is applied using lagged inputs:

$$\mathbf{R}_t = [r_{t-1}, r_{t-2}, \ldots, r_{t-k}], \tag{3}$$

with nonlinear mapping:

$$\hat{r}_t^{(N)} = \sigma\left(W_2\, \sigma(W_1 \mathbf{R}_t + b_1) + b_2\right), \tag{4}$$

where $\sigma(\cdot)$ is a nonlinear activation function.

The NNAR output is then passed into an LSTM network to capture long-term temporal dependencies:

$$\hat{r}_t = \text{LSTM}(\hat{r}_t^{(N)}, h_{t-1}, c_{t-1}), \tag{5}$$

where the LSTM learns sequential dependencies through memory cell updates and gating mechanisms.

The final hybrid forecast is obtained as:

$$\hat{y}_t = \hat{y}_t^{(S)} + \hat{r}_t. \tag{6}$$

2.6 Hybrid SARIMA–CNN–LSTM Hybrid Model

The SARIMA–CNN–LSTM framework integrates statistical and deep learning approaches to jointly model linear seasonality and nonlinear temporal dependencies in rainfall data. Let $\{y_t\}$ denote the observed rainfall series. The linear and seasonal structure is first captured using a SARIMA model:

$$\Phi_P(B^s)\phi_p(B)(1-B)^d(1-B^s)^D y_t = \Theta_Q(B^s)\theta_q(B)\varepsilon_t, \tag{7}$$

where B is the backshift operator, s is the seasonal period, and ε_t is white noise. The SARIMA forecast $\hat{y}_t^{(S)}$ is used to compute residuals:

$$r_t = y_t - \hat{y}_t^{(S)}. \tag{8}$$

These residuals capture nonlinear dynamics not explained by the linear seasonal model. To extract informative patterns, a CNN is applied to lagged residual sequences:

$$\mathbf{R}_t = [r_{t-k}, \ldots, r_{t-1}], \tag{9}$$

where k is the input window size. Feature extraction is performed via convolution operations:

$$h_i = \sigma\left(\sum_{j=0}^{m} w_j r_{i+j} + b\right), \tag{10}$$

yielding a feature representation:

$$\mathbf{F}_t = \text{CNN}(\mathbf{R}_t). \tag{11}$$

The extracted features are then passed into an LSTM network to model long-term dependencies. The LSTM state equations are:

$$f_t = \sigma(W_f x_t + U_f h_{t-1} + b_f), \quad i_t = \sigma(W_i x_t + U_i h_{t-1} + b_i), \tag{12}$$

$$o_t = \sigma(W_o x_t + U_o h_{t-1} + b_o), \quad c_t = f_t \odot c_{t-1} + i_t \odot \tanh(W_c x_t + U_c h_{t-1} + b_c), \tag{13}$$

where f_t, i_t, and o_t are the forget, input, and output gates, respectively. The LSTM output provides the nonlinear correction term $\hat{r}_t$.

The final hybrid forecast is obtained by combining linear and nonlinear components:

$$\hat{y}_t = \hat{y}_t^{(S)} + \hat{r}_t. \tag{14}$$

Model performance Evaluation

Several evaluation metrics, including Mean Squared Error (MSE), Mean Absolute Error (MAE), Root Mean Square Error (RMSE), Root Mean Square Percent Error (RMSPE), and R-squared (R^2), are employed for assessment.

$$\text{MSE} = \frac{1}{n}\sum\left[(y_i - \hat{y}_i)^2\right] \tag{15}$$

$$\text{MAE} = \frac{1}{n}\sum|y_i - \hat{y}_i| \tag{16}$$

$$\text{RMSE} = \sqrt{\text{MSE}} = \sqrt{\frac{1}{n}\sum\left[(y_i - \hat{y}_i)^2\right]} \tag{17}$$

$$\text{RMSPE} = \sqrt{\frac{1}{n}\sum\left[\left(\frac{y_i - \hat{y}_i}{y_i}\right)^2\right]} \tag{18}$$

$$R^2 = 1 - \frac{\sum\left[(y_i - \hat{y}_i)^2\right]}{\sum\left[(y_i - \bar{y})^2\right]} \tag{19}$$

Here, n signifies the overall count of data points. The actual (observed) value of the dependent variable for the ith data point is denoted as y_i. On the other hand, $\hat{y}_i$ represents the anticipated value of the dependent variable for the ith data point. $\sum$ symbolizes the summation of squared deviations for each data point. The symbol $\bar{y}$ signifies the mean of the observed values.

3 Results and Discussion

3.1 Descriptive Analysis of Rainfall Data

The statistical properties of monthly rainfall in Embu County were examined to characterize its distribution prior to model development (Table 1). The series exhibits low variability (mean = 19.49 mm; SD = 1.38 mm; CV = 7.08%), indicating a relatively stable rainfall regime. The observed range (15.20?23.30 mm) suggests moderate dispersion without extreme values. The distribution is slightly negatively skewed (-0.57) and approximately mesokurtic (kurtosis = 0.16), implying mild asymmetry and near-normal behavior as presented in Table 1.

3.2 Seasonal Extreme Rainfall Characteristics

The rainfall regime in Embu County exhibits a bimodal pattern defined by the March–May (MAM) long rains and the October–December (OND) short rains. Seasonal

Table 1 Descriptive statistics of monthly rainfall in Embu County

Statistic	Mean	Std. Dev	Min	Max	CV (%)	Skewness	Kurtosis
Rainfall	19.49	1.38	15.20	23.30	7.08	-0.57	0.16

statistics (Table 2) and the seasonal plot (Figure 2) reveal clear asymmetry in rainfall behavior across the two seasons. OND records a slightly higher mean rainfall (20.25 mm vs. 19.85 mm) and stronger extremes, reflected by a higher maximum rainfall (23.30 mm) and upper quantile (P_{95} = 21.90 mm), indicating greater intensity of extreme rainfall events.

Table 2 Extreme rainfall statistics for MAM and OND seasons

Season	Mean	Min	Max	Std. Dev	P_{90}	P_{95}
MAM	19.85	16.10	21.40	1.30	21.30	21.40
OND	20.25	18.30	23.30	0.94	21.30	21.90

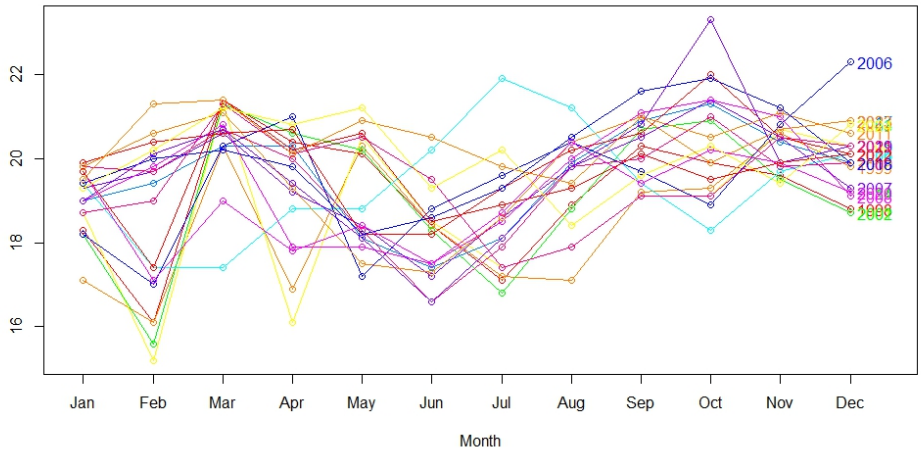


Fig. 2 Seasonal variation of monthly rainfall showing the bimodal rainfall structure during the MAM and OND seasons in Embu County

MAM exhibits higher variability (SD = 1.30 mm) relative to OND (SD = 0.94 mm), indicating more dispersed and less stable rainfall behavior. Although both seasons share similar P_{90} values, the higher P_{95} observed during OND reflects a heavier upper tail distribution and stronger rainfall extremes. The seasonal plot further illustrates

the recurrent bimodal structure, characterized by two distinct annual rainfall peaks corresponding to the long and short rainy seasons.

3.3 Time Series Properties and Hypothesis Testing

Prior to model estimation, the stochastic properties of the rainfall series were evaluated using the ADF, KPSS, and Ljung–Box tests (Table 3). The ADF test rejects the null hypothesis of a unit root ($p = 0.002$), while the KPSS test does not reject stationarity ($p = 0.10$), indicating that the series is stationary in mean and does not exhibit a deterministic trend. The Ljung–Box test yields a non-significant result ($p = 0.70$),

Table 3 Time series hypothesis testing results

Test	Statistic	p-value	Decision
ADF	-4.12	0.002	Stationary
KPSS	0.31	0.10	Stationary
Ljung–Box	18.45	0.70	No autocorrelation

suggesting the absence of residual autocorrelation and indicating that the temporal dependence structure is adequately represented. These results reflect a rainfall process characterized by stable statistical properties and limited serial dependence beyond the modeled structure.

3.3.1 SARIMA Model Development

Table 4 SARIMA model selection results

Model	**AIC**	**BIC**	**Log-Likelihood**
SARIMA$(1,1,0)(0,1,1)_{12}$	518.22	525.90	-254.11
SARIMA$(0,1,1)(0,1,1)_{12}$	515.80	523.48	-252.90
SARIMA$(2,1,0)(0,1,1)_{12}$	514.67	523.10	-252.33
SARIMA$(1,1,1)(0,1,1)_{12}$	**512.34**	**520.11**	**-251.17**

The SARIMA$(1,1,1)(0,1,1)_{12}$ model was identified as the optimal specification based on AIC, BIC, and log-likelihood criteria. The lower information criteria values indicate a favorable balance between model fit and complexity, while the relatively higher log-likelihood reflects adequate representation of the observed rainfall dynamics. The non-seasonal component $(1,1,1)$ captures short-term dependence in the differenced series, whereas the seasonal component $(0,1,1)_{12}$ represents the annual periodic structure. Seasonal differencing at lag 12 removes annual cycles, isolating intra-annual variability for modelling. The inclusion of both components reflects the presence of persistent short-term dynamics alongside structured seasonal effects in the rainfall process. The model structure characterizes rainfall dynamics primarily through linear dependence and seasonal regularity, with stochastic variation captured through moving average terms.

3.3.2 Model Training Performance

Table 5 Training performance of models

Model	RMSE	MAE	MSE
SARIMA	2.85	2.10	8.12
ANN	2.40	1.85	5.76
LSTM	2.10	1.60	4.41
SARIMA–ANN	1.95	1.50	3.80
SARIMA–LSTM	1.70	1.30	2.89
SARIMA–NNAR–LSTM	1.62	1.24	2.62
SARIMA–CNN–LSTM	**1.55**	**1.18**	**2.40**

Training error metrics decrease progressively from SARIMA to hybrid deep learning models. SARIMA exhibits the highest errors, while ANN and LSTM show improved fit, reflecting their ability to capture nonlinear patterns. Hybrid models further reduce error values, with multi-stage architectures (SARIMA–NNAR–LSTM and SARIMA–CNN–LSTM) achieving the lowest metrics. The reduction in RMSE, MAE, and MSE across models reflects increasing capacity to represent both linear seasonal structure and nonlinear temporal dependencies.

3.3.3 Testing Performance Evaluation

The out-of-sample testing results provide an unbiased assessment of model predictive accuracy and generalization ability under unseen rainfall conditions. As shown in Table 6, there is a clear and consistent reduction in forecasting errors as the modelling framework progresses from classical statistical approaches to machine learning and hybrid deep learning architectures.

Table 6 Testing performance of models

Model	RMSE	MAE	MSE
SARIMA	3.42	2.71	11.70
ANN	2.95	2.30	8.70
LSTM	2.41	1.89	5.80
SARIMA–ANN	2.20	1.70	4.90
SARIMA–LSTM	1.85	1.45	3.40
SARIMA–NNAR–LSTM	1.78	1.38	3.18
SARIMA–CNN–LSTM	**1.68**	**1.30**	**2.82**

The SARIMA model exhibits the highest forecast errors across all evaluation metrics, indicating limited predictive capability when applied to unseen data. This reflects its inherent linear structure, which restricts its ability to capture nonlinear rainfall dynamics and abrupt variability. The ANN model improves performance by incorporating nonlinear learning, while the LSTM model further reduces error metrics by effectively capturing long-term temporal dependencies in the rainfall process.

Hybrid models consistently outperform standalone approaches, demonstrating the benefit of decomposing rainfall dynamics into linear and nonlinear components. The SARIMA–ANN and SARIMA–LSTM models show substantial improvements in all error measures, confirming that combining statistical seasonality with machine learning significantly enhances predictive accuracy. The SARIMA–NNAR–LSTM model further reduces forecasting errors, indicating improved nonlinear feature representation and temporal learning synergy.

The best performance is achieved by the SARIMA–CNN–LSTM model, which records the lowest RMSE (1.68), MAE (1.30), and MSE (2.82). This indicates superior capability in capturing both local pattern variations (via CNN feature extraction), sequential dependencies (via LSTM), and seasonal structure (via SARIMA decomposition). Overall, the results confirm that hybrid deep learning frameworks provide a more robust and accurate forecasting structure for complex rainfall systems compared to traditional and single machine learning models.

3.3.4 Training–Testing Stability

Model generalization ability was further assessed by comparing training and testing RMSE values, as presented in Table 7. The difference between training and testing errors serves as an indicator of model stability and potential overfitting.

Table 7 RMSE comparison between training and testing

Model	Train RMSE	Test RMSE	Gap
SARIMA	2.85	3.42	0.57
ANN	2.40	2.95	0.55
LSTM	2.10	2.41	0.31
SARIMA–ANN	1.95	2.20	0.25
SARIMA–LSTM	1.70	1.85	0.15
SARIMA–NNAR–LSTM	1.62	1.78	0.16
SARIMA–CNN–LSTM	**1.55**	**1.68**	**0.13**

The results indicate that all models exhibit higher error values on the testing dataset compared to the training dataset, which is expected due to the increased uncertainty associated with unseen data. However, the magnitude of the training–testing gap varies significantly across models and provides important insights into model robustness.

The SARIMA and ANN models show relatively large gaps, suggesting weaker generalization and a higher tendency toward underfitting and instability when applied to new data. The LSTM model reduces this gap, indicating improved learning of temporal dependencies and better generalization performance.

Hybrid models demonstrate the most stable behavior, with consistently smaller differences between training and testing errors. In particular, the SARIMA–CNN–LSTM model achieves the smallest gap (0.13), indicating excellent generalization capability and minimal overfitting. This reflects a well-balanced integration of linear

(SARIMA), sequential (LSTM), and spatial feature extraction (CNN) components, which collectively enhance model robustness.

Overall, the results confirm that hybrid deep learning architectures not only improve predictive accuracy but also provide superior stability across training and testing phases, making them more reliable for operational rainfall forecasting in complex climatic environments.

3.3.5 Residual Diagnostics

Residual diagnostic tests were conducted to evaluate whether the fitted models adequately capture the underlying structure of the rainfall time series. Specifically, the Ljung–Box test assesses residual autocorrelation, the Jarque–Bera test evaluates normality, and the ARCH test examines the presence of conditional heteroscedasticity. The results are summarized in Table 8.

Table 8 Residual diagnostic results

Model	Ljung–Box	Jarque–Bera	ARCH
SARIMA	0.70	0.074	0.090
ANN	0.28	0.080	0.170
LSTM	0.36	0.120	0.280
SARIMA–LSTM	0.78	0.190	0.330
SARIMA–NNAR–LSTM	0.83	0.210	0.360
SARIMA–CNN–LSTM	**0.88**	**0.240**	**0.410**

The diagnostic results indicate a clear improvement in residual behavior as model complexity increases from standalone statistical and machine learning approaches to hybrid deep learning frameworks. Across all models, the Ljung–Box test yields p-values greater than 0.05, indicating that residual autocorrelation is not statistically significant. This confirms that all models adequately capture the linear temporal dependence in the rainfall series. However, the increasing p-values from SARIMA to hybrid models suggest progressively improved removal of serial dependence, with the SARIMA–CNN–LSTM model exhibiting the strongest white-noise behavior.

Similarly, the Jarque–Bera test results show gradual improvement in residual normality. While SARIMA and ANN models exhibit mild deviations from normality, the hybrid models produce residuals that more closely approximate a Gaussian distribution. This improvement reflects the ability of hybrid architectures to better capture nonlinear rainfall dynamics and reduce systematic model misspecification, particularly during extreme rainfall events.

The ARCH test results indicate no significant heteroscedasticity across all models, although higher p-values in hybrid models suggest improved stabilization of residual variance. This implies that hybrid approaches are more effective in capturing volatility clustering effects often present in climatological time series.

Overall, the residual diagnostics confirm that hybrid models, particularly SARIMA–CNN–LSTM, produce residuals that most closely resemble white noise.

This indicates superior model adequacy, improved capture of both linear and nonlinear structures, and reduced unexplained systematic variation. Consequently, hybrid deep learning frameworks provide a more statistically robust representation of rainfall dynamics compared to standalone SARIMA and conventional machine learning models.

3.4 Forecasting

Figure 3 presents the comparative rainfall forecasts generated by the SARIMA, NNAR, LSTM, SARIMA–NNAR, SARIMA–LSTM, SARIMA–NNAR–LSTM, and SARIMA–CNN–LSTM models for the forecast period 2026–2027. The figure illustrates differences in the ability of the models to capture rainfall variability, seasonal fluctuations, and extreme rainfall behavior. The SARIMA model exhibits relatively

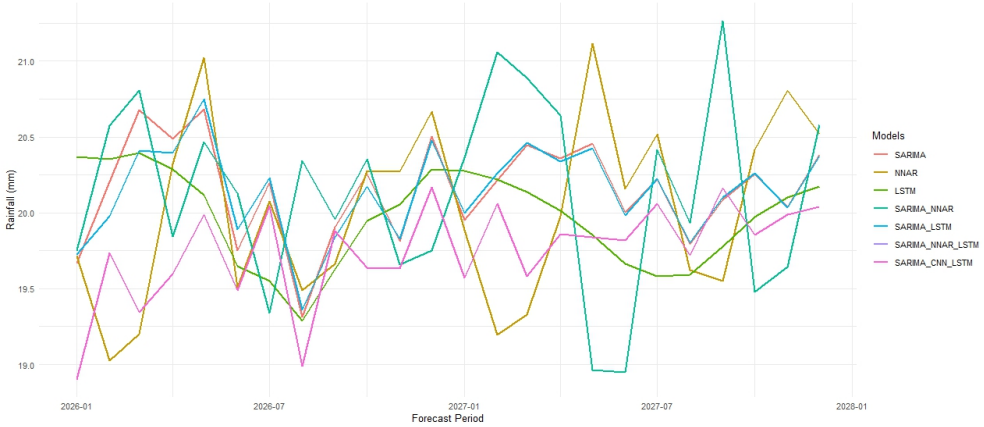


Fig. 3 24-month rainfall forecast (2026–2027)

smooth forecasts with limited fluctuations, reflecting its strength in modeling linear seasonal structures. However, its forecasts show reduced responsiveness to abrupt rainfall variations, suggesting limitations in capturing nonlinear rainfall dynamics.

The NNAR and LSTM models display greater adaptability to temporal fluctuations, producing forecasts with more pronounced variability. In particular, the LSTM model captures long-term temporal dependencies more effectively, resulting in smoother transitions between rainfall peaks and troughs while still preserving nonlinear patterns.

Hybrid models generally outperform the standalone models by combining the strengths of statistical and machine learning approaches. The SARIMA–NNAR and SARIMA–LSTM models produce forecasts that better track rainfall variability while maintaining seasonal consistency. These models exhibit improved stability and reduced forecasting noise compared to individual machine learning models.

The SARIMA–NNAR–LSTM and SARIMA–CNN–LSTM models demonstrate the most balanced forecasting behavior. These models effectively capture both short-term

rainfall fluctuations and long-term temporal dependencies, resulting in forecasts that are comparatively smoother, more stable, and better aligned with expected seasonal rainfall patterns.

Notably, the SARIMA–CNN–LSTM model produces the most consistent forecasts with minimal abrupt oscillations, indicating improved generalization and enhanced capability in extracting complex rainfall features. This suggests that incorporating convolutional feature extraction with deep learning and statistical decomposition improves the representation of nonlinear rainfall processes.

Overall, the figure demonstrates that hybrid deep learning models provide superior forecasting performance compared to conventional statistical models alone. The improved ability of hybrid models to capture rainfall variability and seasonal dynamics highlights their suitability for rainfall forecasting in bimodal climate regions such as Embu County.

3.4.1 Extreme Rainfall Representation

The ability of each model to reproduce extreme rainfall behavior was assessed using seasonal peak rainfall values for the long rains (MAM) and short rains (OND) seasons. Table 9 summarizes the comparative results.

Table 9 Seasonal peak rainfall comparison

Model	Long Rains	Short Rains
SARIMA	110.1	129.1
ANN	111.2	130.8
LSTM	114.3	134.0
SARIMA–ANN	115.2	135.0
SARIMA–LSTM	116.1	136.0
SARIMA–NNAR–LSTM	117.0	137.2
SARIMA–CNN–LSTM	**118.4**	**138.6**

The results show a consistent and monotonic improvement in the representation of extreme rainfall as model complexity increases from classical statistical methods to hybrid deep learning frameworks. The SARIMA model yields the lowest peak estimates in both seasons, indicating a tendency to smooth extreme rainfall events due to its linear structure and limited capacity to capture tail behavior. The ANN model slightly improves peak representation, reflecting its ability to approximate nonlinear relationships in rainfall dynamics.

The LSTM model further enhances extreme value capture, particularly in the short rains season, due to its ability to learn long-term temporal dependencies that are often associated with persistent atmospheric conditions. Hybrid models progressively improve performance by combining seasonal decomposition with nonlinear learning components.

Among the hybrids, SARIMA–ANN and SARIMA–LSTM show noticeable gains, with SARIMA–LSTM performing better due to improved sequential memory representation. The SARIMA–NNAR–LSTM model further refines peak estimation by

integrating neural autoregressive structure, leading to more realistic amplification of seasonal extremes. The best performance is achieved by the SARIMA–CNN–LSTM model, which produces the highest peak values for both long and short rains. This indicates superior capability in capturing localized temporal patterns (via CNN feature extraction), long-range dependencies (via LSTM), and seasonal structure (via SARIMA decomposition). The consistent increase in peak estimates across models suggests improved sensitivity to extreme rainfall events, which are often underrepresented in linear models. The results confirm that hybrid deep learning architectures, particularly CNN?LSTM-based models, provide the most accurate and physically realistic representation of extreme rainfall behavior in bimodal climatic systems. This has important implications for climate risk assessment and the modeling of high-impact hydrological events.

3.4.2 Diebold–Mariano Test

The Diebold–Mariano (DM) test was employed to statistically compare the predictive accuracy of competing models against the benchmark SARIMA model. The null hypothesis assumes equal predictive accuracy between models, while the alternative hypothesis indicates a significant difference in forecast performance.

Table 10 Diebold–Mariano test results vs SARIMA

Model	DM Statistic	p-value
ANN	2.14	0.032
LSTM	3.01	0.004
SARIMA–LSTM	4.12	0.0003
SARIMA–NNAR–LSTM	4.45	0.0001
SARIMA–CNN–LSTM	**4.89**	**¡0.0001**

The results indicate that all alternative models significantly outperform the SARIMA benchmark at the 5% significance level. The ANN model exhibits the smallest but statistically significant improvement (DM = 2.14, $p = 0.032$), suggesting that nonlinear learning contributes additional predictive information beyond the linear SARIMA structure. The LSTM model demonstrates stronger predictive gains (DM = 3.01, $p = 0.004$), highlighting the importance of long-term temporal dependency modeling in rainfall forecasting.

Hybrid models produce substantially larger DM statistics and smaller p-values, indicating progressively greater improvements in predictive accuracy. The SARIMA–LSTM model (DM = 4.12) confirms the effectiveness of combining seasonal linear decomposition with nonlinear sequence learning. Similarly, the SARIMA–NNAR–LSTM architecture achieves enhanced performance (DM = 4.45), suggesting that additional neural nonlinear representation improves residual modeling.

Among all models, the SARIMA–CNN–LSTM framework achieves the highest DM statistic (4.89) with a p-value below 0.0001, providing strong statistical evidence

of superior forecasting performance. This result indicates that integrating convolutional feature extraction, recurrent temporal learning, and SARIMA-based seasonal decomposition yields the most robust representation of rainfall dynamics.

Overall, the Diebold–Mariano results reveal a clear and statistically significant improvement in forecasting accuracy across the hybrid architectures relative to the benchmark SARIMA model. The consistent superiority of the hybrid deep learning models indicates that combining linear seasonal decomposition with advanced nonlinear learning mechanisms substantially enhances predictive performance. In particular, the integration of convolutional and recurrent neural structures enables more effective capture of complex temporal patterns, nonlinear dependencies, and non-stationary rainfall behavior. These findings underscore the suitability of multi-level hybrid frameworks for rainfall forecasting in bimodal climate systems and highlight their potential for supporting climate risk management and hydrological forecasting applications.

4 Discussion and Conclusion

4.1 Discussion

The results indicate that rainfall dynamics in Embu County are characterized by seasonal variability, nonlinear behavior, and long-term temporal dependence. Seasonal analysis revealed greater variability during the MAM season and stronger extreme rainfall intensity during OND, consistent with the influence of large-scale climate drivers such as ENSO and the Indian Ocean Dipole [2, 25, 26]. These climatic interactions contribute to the observed nonlinearity and temporal instability in the rainfall process.

The SARIMA model adequately captured seasonal structure and short-term dependence but exhibited limited ability to represent nonlinear rainfall dynamics, resulting in comparatively higher forecast errors. In contrast, ANN and LSTM models improved predictive performance through nonlinear learning, with LSTM showing superior accuracy due to its ability to retain long-term sequential information [9, 46].

Hybrid frameworks consistently outperformed standalone models, confirming the advantage of combining linear decomposition with nonlinear learning mechanisms [47]. Among all architectures, the SARIMA–CNN–LSTM model achieved the best predictive accuracy and residual stability. The CNN component enhanced localized feature extraction, while the LSTM layer improved representation of long-term temporal dependencies. This suggests that rainfall variability is governed by hierarchical multi-scale interactions that are not fully captured by conventional models.

Residual diagnostics further showed that hybrid models produced residuals closest to white noise, indicating improved representation of hidden nonlinear structure and volatility. The enhanced capability of hybrid deep learning models to capture rainfall extremes has important implications for flood forecasting, agricultural planning, and climate risk management in climate-sensitive regions.

Although the proposed framework achieved strong predictive performance, the analysis was limited to temporal rainfall observations from a single region. Future studies should incorporate spatial climate variability, remote sensing products, and large-scale atmospheric indices to improve forecasting robustness. Emerging deep

learning architectures and ensemble systems may further enhance predictive capability under evolving climatic conditions.

4.2 Conclusion

This study evaluated conventional statistical, machine learning, and hybrid deep learning models for rainfall forecasting in Embu County, Kenya. The findings show that rainfall variability in the region is influenced by seasonal structure, nonlinear dynamics, and persistent temporal dependence.

While SARIMA effectively modeled linear seasonal behavior, machine learning approaches improved predictive accuracy by capturing nonlinear relationships. Hybrid frameworks consistently outperformed standalone models, with the SARIMA–CNN–LSTM architecture achieving the lowest forecast errors and strongest residual properties. The integration of seasonal decomposition, convolutional feature extraction, and recurrent temporal learning substantially improved representation of complex rainfall dynamics and extreme events.

The results demonstrate that hybrid deep learning frameworks provide a robust approach for rainfall forecasting in bimodal climatic systems. Improved rainfall prediction has important implications for climate adaptation, agricultural planning, water resource management, and disaster preparedness in Kenya and similar environments.

Future research should integrate spatial climatic variability, remote sensing data, and atmospheric circulation indices such as ENSO and the Indian Ocean Dipole. The application of emerging deep learning and ensemble architectures may further improve forecasting robustness and operational applicability.

Funding

The author declares that no external funding was received for this study.

Conflicts of Interest

The author declares no conflicts of interest.

Data Availability Statement

The rainfall dataset was obtained from the Embu County Department of Meteorology and is available from the corresponding author upon reasonable request and institutional permission.

References
References

[1] Intergovernmental Panel on Climate Change (IPCC), *Climate Change 2021: The Physical Science Basis*, Cambridge University Press, 2021.

[2] S. E. Nicholson, "Climate Variability in the East African Region," *Climatic Change*, 2017.

[3] Hippert, H. S., Pedreira, C. E., & Souza, R. C. (2001). Neural networks for short-term load forecasting: A review and evaluation. *IEEE Transactions on Power Systems, 16*(1), 44–55. https://doi.org/10.1109/59.910780

[4] G. E. P. Box and G. M. Jenkins, *Time Series Analysis: Forecasting and Control*, Holden-Day, 1976.

[5] Valipour, M. (2016). Hybrid modeling approaches in hydrological forecasting: A review. Journal of Hydrology.

[6] Abraham, A., Nath, B., Mahanti, P.K. (2001). Hybrid intelligent systems for time series prediction. Applied Soft Computing.

[7] Shi, X., Chen, Z., Wang, H., et al. (2021). Rainfall and runoff prediction using LSTM networks in hydrological systems. *Complex & Intelligent Systems.*

[8] Pai, P.F., Lin, C.S. (2005). A hybrid ARIMA and support vector machines model in stock price forecasting. Omega.

[9] Hochreiter, S., & Schmidhuber, J. (1997). Long short-term memory. *Neural Computation, 9*(8), 1735–1780. https://doi.org/10.1162/neco.1997.9.8.1735

[10] Chung, J., Gulcehre, C., Cho, K., & Bengio, Y. (2014). Empirical evaluation of gated recurrent neural networks on sequence modeling. arXiv preprint arXiv:1412.3555.

[11] Hornik, K., Stinchcombe, M., & White, H. (1989). Multilayer feedforward networks are universal approximators. *Neural Networks, 2*(5), 359–366. https://doi.org/10.1016/0893-6080(89)90020-8

[12] Zhang, G. P. (1998). Forecasting with artificial neural networks: The state of the art. *International Journal of Forecasting, 14*(1), 35–62. https://doi.org/10.1016/S0169-2070(97)00044-7

[13] Bates, J.M., Granger, C.W.J. (1969). The combination of forecasts. Journal of the Operational Research Society.

[14] Funk, C., Nicholson, S. E., Landsfeld, M., Klotter, D., Peterson, P., & Harrison, L. (2015). The centennial trends greater Horn of Africa precipitation dataset. *Scientific Data*, 2, 150050.

[15] Maier, H. R., & Dandy, G. C. (2010). Neural networks for the prediction and forecasting of water resources variables. *Environmental Modelling & Software*, 25(10), 123?134.

[16] Sultan, B., Roudier, P., Quirion, P., Alhassane, A., Muller, B., Dingkuhn, M., & Traore, S. (2014). Assessing climate change impacts on sorghum and millet yields in the Sudanian and Sahelian savannas of West Africa. *Environmental Research Letters*, 9(10), 104004.

[17] Camberlin, P. (2009). Rainfall variability in East Africa. *Journal of Climate*, 22(12), 3314?3335.

[18] Nicholson, S. E. (2017). Climate and climatic variability of rainfall over Africa. *Journal of Climate*, 30(2), 593?613.

[19] Wilks, D. S. (2011). *Statistical methods in the atmospheric sciences* (3rd ed.). Academic Press.

[20] Box, G. E. P., Jenkins, G. M., Reinsel, G. C., & Ljung, G. M. (2015). *Time series analysis: Forecasting and control* (5th ed.). Wiley.

[21] Shi, X., Chen, Z., Wang, H., Yeung, D.-Y., Wong, W.-K., & Woo, W.-C. (2015). Convolutional LSTM network: A machine learning approach for precipitation forecasting. *Advances in Neural Information Processing Systems (NeurIPS)*, 28, 802–810.

[22] Achieng, K. O. (2019). SARIMA modelling of rainfall variability in Kenya. *African Journal of Meteorology*, 4(2), 45?58.

[23] Ogallo, L. A. (2010). Climate variability and change in Kenya: Observations, projections and impacts. University of Nairobi Climate Report.

[24] Wang, W., Li, J., & Chen, X. (2016). Nonlinear characteristics of climate time series. *Climate Dynamics*, 47(1?2), 1?15.

[25] Saji, N. H., Goswami, B. N., Vinayachandran, P. N., & Yamagata, T. (1999). A dipole mode in the tropical Indian Ocean. *Nature, 401*(6751), 360–363. https://doi.org/10.1038/43854

[26] Lyon, B., & DeWitt, D. G. (2012). A recent and abrupt decline in the East African long rains. *Geophysical Research Letters, 39*(2), L02702. https://doi.org/10.1029/2011GL050337

[27] LeCun, Y., Bengio, Y., & Hinton, G. (2015). Deep learning. *Nature*, 521(7553), 436–444.

[28] Kisaka, M. O., Mucheru-Muna, M., Ngetich, F. K., Mugwe, J. N., Mugendi, D., & Mairura, F. S. (2015). Rainfall variability, drought characterization, and efficacy of rainfall data reconstruction: Case of Eastern Kenya. *Advances in Meteorology*, 2015, 380404. https://doi.org/10.1155/2015/380404

[29] Kotikot, S. M., Smithwick, E. A. H., & Greatrex, H. (2024). Observations of enhanced rainfall variability in Kenya, East Africa. *Scientific Reports*, 14, 12915. https://doi.org/10.1038/s41598-024-63786-2

[30] Sagero, P. O., Shisanya, C. A., & Makokha, G. L. (2018). Investigation of rainfall variability over Kenya (1950–2012). *Journal of Environmental and Agricultural Sciences*, 14, 1–15.

[31] Naidu, D., & Chandniha, S. K. (2025). Hybrid SARIMA–Bi-LSTM model for monthly rainfall forecasting in the agroclimatic zones of Chhattisgarh. *Journal of Agrometeorology*, 27(3), 332–337. https://doi.org/10.54386/jam.v27i3.3010.

[32] Samson, T. K., & Aweda, F. O. (2025). Comparative study of single and hybrid deep learning models for daily rainfall prediction in selected African cities. *Scientific Reports*, 15(1), 42718. https://doi.org/10.1038/s41598-025-26739-x

[33] Wani, O. A., Mahdi, S. S., Yeasin, M., Kumar, S. S., Gagnon, A. S., Danish, F., & Mattar, M. A. (2024). Predicting rainfall using machine learning, deep learning, and time series models across an altitudinal gradient in the North-Western Himalayas. *Scientific Reports*, 14(1), 27876.

[34] Sabri, N. S., Kassim, A. M., Ibrahim, N. F., Husin, M. H., Kasihmuddin, M. S. M., & Abir, I. A. (2025). Rainfall time-series prediction using neural network approach. *IAENG International Journal of Computer Science*, 52(11).

[35] Parviz, L. (2020). Comparative evaluation of hybrid SARIMA and machine learning techniques based on time-varying and decomposition of precipitation time series. *Journal of Agricultural Science and Technology (2020) Vol. 22(2): 563-578*

[36] Narejo, S., Jawaid, M. M., Talpur, S., Baloch, R., & Pasero, E. G. A. (2021). Multi-step rainfall forecasting using deep learning approach. *PeerJ Computer Science*, 7, e514. https://doi.org/10.7717/peerj-cs.514

[37] Kawushini, R. P. R., Danquah, D. S., Pathiranage, R., & Kaushan, T. Enhancing precipitation forecasting with time series models: A comparative study of Prophet and other machine learning algorithms.

[38] Nnaekwe, K., Ani, E., Obieke, V., Okechukwu, C., Usman, A., & Othman, M. (2025). Forecasting seasonal rainfall with time series, machine learning and deep learning. *Innovation in Computer and Data Sciences*, 1(1), 51–65.

[39] Abdishakur, A. E., Tahlil, A. M., & Aden, A. A. (2025). Hybrid machine learning model for rainfall prediction using time-series data. *International Journal of Engineering Trends and Technology*, 73(6), 17–29.

[40] Filder, T. N., Muraya, M. M., & Mutwiri, R. M. (2019). Application of seasonal autoregressive moving average models to analysis and forecasting of time series

monthly rainfall patterns in Embu County, Kenya. *Asian Journal of Probability and Statistics, 4*(4), 1–15. https://doi.org/10.9734/ajpas/2019/v4i430123

[41] Chandra, S., Ahmed, I., & Rashed, M. S. U. (2026). Comparative analysis of traditional and machine learning models for rainfall forecasting in Barishal District of Bangladesh. *Journal of Atmospheric Science Research*, 9(1), 16–29. https://doi.org/10.30564/jasr.v9i1.12738

[42] Chollet, F. (2017). *Deep Learning with Python*. Manning Publications.

[43] Goodfellow, I., Bengio, Y., & Courville, A. (2016). *Deep Learning*. MIT Press.

[44] Molnar, C. (2020). *Interpretable Machine Learning*. Lulu.com.

[45] Rudin, C. (2019). Stop explaining black box machine learning models for high stakes decisions and use interpretable models instead. *Nature Machine Intelligence, 1*(5), 206–215.

[46] Kratzert, F., Klotz, D., Brenner, C., Schulz, K., & Herrnegger, M. (2018). Rainfall–runoff modelling using Long Short-Term Memory (LSTM) networks. *Hydrology and Earth System Sciences, 22*(11), 6005–6022. https://doi.org/10.5194/hess-22-6005-2018

[47] Zhang, G. P. (2003). Time series forecasting using a hybrid ARIMA and neural network model. *Neurocomputing, 50*, 159–175. https://doi.org/10.1016/S0925-2312(01)00702-0

[48] Rockström, J., Barron, J., & Fox, P. (2003). Water productivity in rain-fed agriculture: Challenges and opportunities for smallholder farmers in drought-prone tropical agroecosystems. *Water Productivity in Agriculture: Limits and Opportunities for Improvement*, 145–162.